NeuroImage: Clinical 27 (2020) 102269

Contents lists available at ScienceDirect

NeuroImage: Clinical

journal homepage: www.elsevier.com/locate/ynicl

Subclinical paranoid beliefs and enhanced neural response during processing of unattractive faces

Stephan Furger[a], Antje Stahnke[a], Francilia Zengaffinen[a], Andrea Federspiel[a], Yosuke Morishima[a], Martina Papmeyer[a], Roland Wiest[b], Thomas Dierks[a], Werner Strik[a,*]

[a] Translational Research Center, University Hospital of Psychiatry, University of Bern, Switzerland
[b] University Institute of Diagnostic and Interventional Neuroradiology, Inselspital, University of Bern, Switzerland

ARTICLE INFO

Keywords:
Face Perception
Dynamic Faces
Paranoid Beliefs
Amygdala
fMRI
SyNoPsis

ABSTRACT

The perception of faces and consequent social inferences are fundamental for interpersonal communication. While facial expression is important for interindividual communication, constitutional and acquired features are crucial for basic emotions of attraction or repulsion. An emotional bias in face processing has been shown in schizophrenia, but the neurobiological mechanisms are unclear. Studies on the interaction between face processing and the emotional state of healthy individuals may help to elucidate the pathogenesis of the paranoid syndrome in psychosis. This study addressed facial attractiveness and paranoid ideas in a non-clinical population. Using functional magnetic resonance imaging (fMRI), we investigated neural activation patterns of 99 healthy subjects during the passive perception of a dynamic presentation of faces with different attractiveness. We found that the perceived attractiveness of faces was linked to the activity of face processing and limbic regions including the fusiform gyrus, amygdala, and prefrontal areas. Paranoid beliefs interacted with perceived attractiveness in these regions resulting in a higher response range and increased activation after the presentation of unattractive faces. However, no behavioral interactions between reported subjective attractiveness and paranoid beliefs were found. The results showed that increased activation of limbic brain regions is linked to paranoid beliefs. Since similar correlations were found in clinical populations with paranoid syndromes, we suggest a dimension of emotional dysregulation ranging from subclinical paranoid beliefs to paranoid schizophrenia.

1. Introduction

Non-verbal communication is essential for adequate social interactions (Jack and Schyns, 2015). Faces are crucial to derive social cues to understand thoughts and intentions and to act accordingly. Facial features lead to judgments about a person (Little et al., 2011), and first impressions are often generalized to draw social inferences (Montepare and Dobish, 2003; Oosterhof and Todorov, 2009; Sutherland et al., 2013). Dynamic facial expressions inform about the emotional state, but constitutional and acquired features such as symmetrical, prototypical or average traits are essential for attraction (Rhodes et al., 2003). Attractiveness is important for social interactions and mating, while disfigurements due to constitution, illness or trauma can dramatically trigger repulsion. Cognitive processing and judgment about facial attractiveness are notoriously controlled by education and social expectancies to protect people with particularly unattractive or attractive faces from discrimination, or harassment, respectively. Yet, asymmetrical faces were perceived as unattractive, and judged to have lower physical health, social competence, power, and intelligence (Rhodes et al., 2001; Zebrowitz et al., 2002; Zebrowitz and Montepare, 2008; Zebrowitz and Rhodes, 2004). Beyond social conventions and expectancies, facial attractiveness has still an important mutual impact in basic emotional communication, mainly in terms of approach and avoidance.

Face perception activates several brain regions involved in visual and emotional processing (Adolphs, 2002; Haxby et al., 2000, 2002). The fusiform gyrus plays a key role in face recognition (Kanwisher et al., 1997; Meaux and Vuilleumier, 2016; Schiltz and Rossion, 2006; Sergent et al., 1992). Several limbic regions, on the other hand, are involved in processing the emotional valence of the perceived face. In particular, the amygdala was involved in processing social salience and relevance, in terms of attractiveness, intention, or trustworthiness (Adolphs, 2010). The amygdala also responded to novel emotional and neutral images containing faces (Balderston et al., 2011), was involved

* Corresponding author.
E-mail address: werner.strik@upd.unibe.ch (W. Strik).

https://doi.org/10.1016/j.nicl.2020.102269
Received 9 December 2019; Received in revised form 2 April 2020; Accepted 20 April 2020
Available online 25 April 2020

in the evaluation of first impressions (Rule et al., 2011), and engaged during the perception of emotional faces (Fitzgerald et al., 2006), in particular if negative and threat-related (Adolphs, 2008; Fusar-poli et al., 2009; Joseph, 2003; Öhman, 2005). Presenting faces with varying attractiveness, increased activation in the medial orbitofrontal cortex (mOFC) was associated with higher facial attractiveness, whereas an increased activation in the lateral orbitofrontal cortex (lOFC) and lateral prefrontal cortex (lPFC) was found for less attractive faces (O'Doherty et al., 2003).

Most studies investigating neural face processing used static pictures as stimuli. Interindividual non-verbal communication in the real world, however, is emphasized by head and eye movements. Dynamic compared to static face stimuli resulted in a more pronounced and widespread activation pattern (Trautmann et al., 2009), and higher arousal (Sato and Yoshikawa, 2007). Furthermore, in healthy populations, dynamic faces elicited an increased neural activity in occipital, temporal, limbic (e.g., amygdala), and prefrontal regions (e.g., inferior frontal gyrus (IFG), and in the middle frontal gyrus (MFG) (Foley et al., 2012; Haxby et al., 2000) compared to static stimuli.

In a long-lasting project of our group, schizophrenia has been defined as a fundamental disorder of interindividual communication, affecting the domains of language, motor behavior and emotions at different extents. Several studies of the last two decades support the hypothesis that these communication domains can be matched to well-described, neuroanatomically, and functionally segregated sensorimotor brain systems, i.e., to the language, executive and limbic system, respectively. In this framework, paranoid syndromes can be defined as an emotional dysregulation with misperceptions of existential threat or supernatural power, and dysfunctional behavioral reactions (Systems Neuroscience of Psychosis: SyNoPsis; Strik et al., 2017 for review). In these syndromes, the perception of the emotional content of prosody and face expression is inaccurate and negatively biased (Bach et al., 2009, 2008). In a similar perspective, Freeman has described a threat-anticipation model which implies multiple causal factors for delusions (Freeman, 2007). In this model, affective processes are at the basis of reasoning biases, jumping to conclusions, and anomalous internal and external experiences that interact with social factors involved in the search for meaning and in persecutory beliefs (Freeman and Garety, 2014).

The SyNoPsis framework is a dimensional model for the psychotic imbalance of the three above mentioned major brain systems involved in higher-order social communication. This predicts a continuum from normal to psychotic for each of these domains. In fact, there is evidence for the limbic domain that unusual beliefs of threat are experienced in the general population (Freeman, 2007) and that these are on a continuum from normal beliefs to persecutory delusional ideas (Freeman, 2006; Linscott and van Os, 2010; Stip and Letourneau, 2009). Studies investigating face processing found impaired emotional perception across the continuum with increasing delusional ideation (Combs et al., 2006). Further, subjects with high levels of non-clinical paranoia showed reduced accuracy for subtle negative emotional expressions and were revealed to have social cognitive and social functioning biases (Combs et al., 2013).

To summarize, research on social perception and clinical characteristics such as delusional ideation with paranoid content is sparse (Mondragón-Maya et al., 2017) and not sufficiently investigated to understand the neurobiological mechanisms (Freeman and Garety, 2014; Murray, 2011). Neurobiologically informed dimensional models may help to understand the mechanisms of emotional perception, processing, and reaction in healthy individuals and psychosis. This is of interest to better understand the nature of psychotic experiences in the general population. Further, this contributes to the question of whether there is a common neurobiological mechanism for subclinical and clinical paranoid ideation. Therefore, the current study aimed to provide further insights into the interaction between face perception and paranoid ideation on the involved face- and emotion-processing brain systems in a non-clinical population. We predicted that dynamic faces would consistently activate the well-known face-decoding areas, including limbic regions, that the subjective evaluation of attractiveness would be related to the hemodynamic response in limbic regions, and that subclinical paranoid ideation would predict the neural reactions to attractive and unattractive faces.

2. Materials and methods

2.1. Participants

We recruited 137 healthy German-speaking participants aged between 16 and 60. A total of 17 participants met at least one of the following exclusion criteria, and were thus excluded from participation: i) history of head injury or loss of consciousness; ii) substance use disorder (except for tobacco), iii) past or current electroconvulsive therapy; iv) current pregnancy/lactating; or v) MRI incompatibility (e.g., metallic structures in body, claustrophobia, etc.). 14 participants were excluded from analyses due to missing data and seven participants due to MRI acquisition failure or bad data quality. This resulted in a final data set of 99 participants. The study was approved by the Ethics Commission of the Canton of Bern (EC-Nr: 2016-01261), and participants gave their written informed consent.

2.2. Experimental procedure

Before study participation, participants were screened via a telephone interview to assess in- and exclusion criteria. Participants eligible for study participation were invited on two non-consecutive examination days for approximately four hours each as several assessments were conducted. The two examination days were in average 17.5 days (SD = 24.1 days, *median* = 9 days) apart. On one of those two examination days, participants completed the MRI measurement. The MRI scan was split into two sessions of each approximately 35 min with a 45-minute break in between, as additional fMRI tasks were performed and to reduce the burden on participants. Among several assessments, participants' handedness was assessed with the Edinburgh Handedness Inventory (EHI) at the beginning of the first examination day. They were grouped into the three categories left-, mixed, and right-handed depending on the total score of the EHI. Paranoid beliefs were assessed with the German version of the 21-item Peters et. al Delusions Inventory (PDI) (Lincoln et al., 2009; Peters et al., 2004), which has been reported to have high test–retest reliability (r = 0.82) and high internal consistency (0.88) (Peters et al., 2004). Participants had to answer if they had diverse unusual beliefs (*yes/no*: number of paranoid beliefs; *possible range*: 0–21) and if yes, how high their levels of conviction, distress, and preoccupation on a scale between 1 and 5 had been (*possible range*: 0–105). Sum scores for each factor and a total sum score (*possible range*: 0 –336) were calculated (Table S1). As expected for a healthy population, the total sum scores were in a lower range with an average of 26.1 (range: 0–117). Since some participants could report low distress for several paranoid beliefs in comparison to participants which could have high distress just for a few paranoid beliefs, we calculated weighted paranoid beliefs scores by dividing the sum scores with the reported number of paranoid beliefs. A summary of the participants demographics and behavioral assessments are shown in Table 1.

2.3. Face perception task

The face perception task consisted of dynamic faces, which were designed to stimulate particularly face processing and limbic brain areas, and to avoid brain activation in regions associated with executive functions (Fig. 1). Participants were instructed to passively look at the dynamic faces and only to react with a button press when a control stimulus appeared.

Table 1
Demographics of the study population.

	Female (N = 75)	Male (N = 24)	Total (N = 99)	Test value	p-value
Age (in years)				2.38	.126
Mean (*SD*)	26.56 (9.36)	30.04 (10.42)	27.40 (9.69)		
Range	16.00–56.00	18.00–58.00	16.00–58.00		
Handedness (EHI)				0.70	.703
left hander	7 (9.3%)	2 (8.3%)	9 (9.1%)		
mixed hander	7 (9.3%)	1 (4.2%)	8 (8.1%)		
right hander	61 (81.3%)	21 (87.5%)	82 (82.8%)		
Paranoid Belief Scores (PDI)					
Number of Paranoid Beliefs				4.26	.042
Mean (*SD*)	3.21 (2.48)	4.62 (4.00)	3.56 (2.96)		
Range	0.00–10.00	0.00–15.00	0.00–15.00		
Conviction (weighted)				2.93	.090
Mean (*SD*)	2.07 (1.18)	2.56 (1.31)	2.19 (1.22)		
Range	0.00–4.00	0.00–5.00	0.00–5.00		
Distress (weighted)				0.63	.429
Mean (*SD*)	1.55 (0.97)	1.38 (0.68)	1.50 (0.90)		
Range	0.00–4.00	0.00–3.00	0.00–4.00		
Preoccupation (weighted)				0.66	.419
Mean (*SD*)	1.57 (0.93)	1.74 (0.87)	1.61 (0.92)		
Range	0.00–3.75	0.00–3.50	0.00–3.75		
Total Score (weighted)				0.66	.419
Mean (*SD*)	6.03 (3.10)	6.60 (2.64)	6.17 (2.99)		
Range	0.00–12.50	0.00–10.50	0.00–12.50		

Note: Differences between female and male participants were assessed by Linear Model ANOVA for numerical data and with Pearson's Chi-squared test for categorical data. The weighted paranoid belief scores were assessed with the Peters et al. Delusions Inventory (PDI) and corrected for the reported number of unusual beliefs. *SD, Standard Deviation; PDI, Peters et al. Delusions Inventory*

For the face perception task, a total of 132 stimuli were used and split into two equal sets for both MRI scan session halves. The stimuli were either dynamic faces, dynamic mosaics (neutral stimuli), or white silhouettes of animals (control stimuli). The face stimuli were 96 short animations (48 per scan session) with variations of four characteristics: *attractiveness* (low or high attractiveness), *gender* (male or female), head *movement* (up or down), and *gaze direction* (direct or averted gaze). After each fixation cross, a face appeared, started in a neutral position, and moved the head either up- or downwards while either keeping eye contact or not. Each dynamic face of the category *attractive* consisted of four faces from the Chicago Face Database (Ma et al., 2015) morphed together to create a symmetrical and more average-looking face. Dynamic faces in the stimuli category *unattractive* consisted of male and female portraits from the photographer Bruce Gilden, who kindly allowed us to modify his images (Bruce Gilden, Faces, Keystone/ Magnum photos). The face stimuli were imported to the FaceGen Modeller (3.12, http://www.facegen.com/) to create 3D models, modified with Adobe Illustrator, and animated with the software FantaMorph (Abrosoft) to create short movie clips with 30 frames per second. The 24 neutral stimuli (12 per session) were animations of scrambled faces in a mosaic pattern where the texture moved either up- or downwards. The 12 control stimuli (six per session) consisted of white static animal

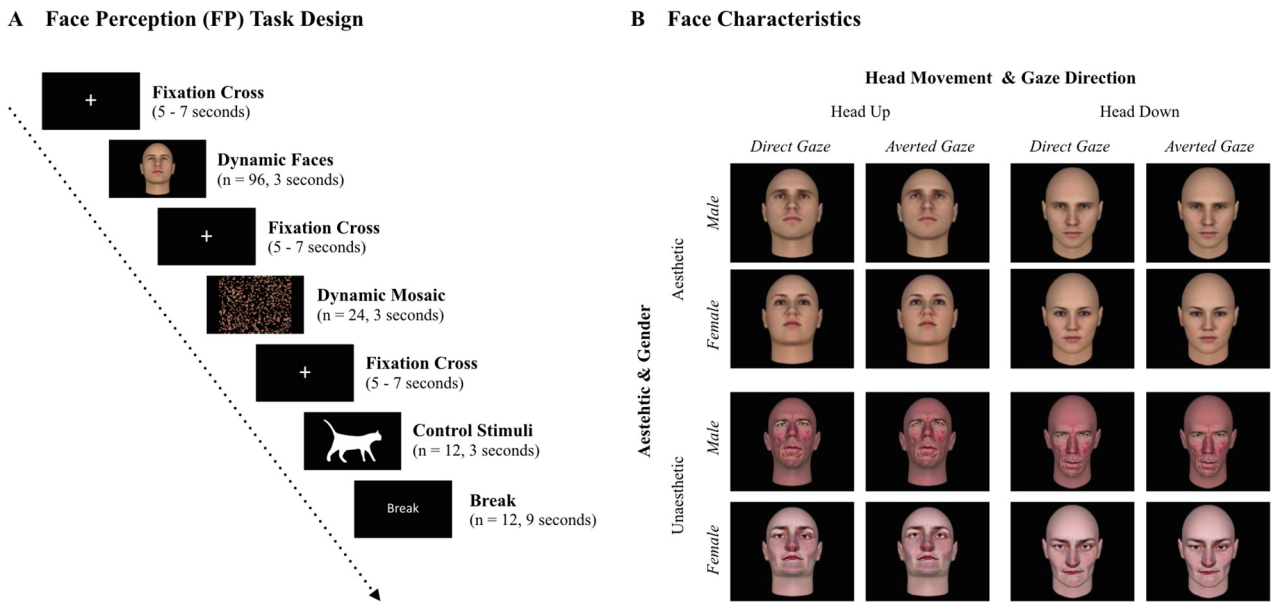

Fig. 1. Experimental design of the face perception task. (A) An illustration of all stimuli and events with the total number and duration in seconds of the task. Stimuli were presented in a pseudo-randomized order and were split into two MRI scan sessions. (B) All possible 16 facial characteristic category combinations of the dynamic face stimuli at the end of the animation. Dynamic faces varied regarding, *attractiveness* (unattractive, attractive) and *gender* (male, female), *head movement* (up, down), and *gaze direction* (direct, averted).

silhouettes (e.g., elephant, bird, dog, etc.). Participants were asked to respond to these control stimuli by pressing a button with their left index finger.

All stimuli were displayed for three seconds followed by a fixation cross with a mean jitter stimulus interval of six seconds (range five to seven seconds) in a pseudo-random event-related design. There were 12 nine-second breaks during the task (six per MRI scan session) with no stimuli presentation. Each session of the FP task in the scanner lasted eleven minutes. To evaluate the dynamic faces, half of the stimuli were randomly presented again on a computer screen outside the MRI scanner at the end of each examination day. Each face was then rated based on perceived attractiveness on a bipolar 7-point Likert scale from −3 (unattractive) to +3 (attractive). PsychoPy version 1.84.2 (Peirce, 2008; Peirce et al., 2019) was used to display the stimuli during MRI acquisition and outside the scanner.

2.4. Behavioral data analysis

Statistical analyses of demographic and behavioral data were performed with R 3.6.1 (R Development Core Team and Development Core Team, 2011) in RStudio (version 1.2.5019). The R package lme4 (Bates et al., 2015) was used for linear mixed-model analysis. Linear model ANOVA for numerical data and Pearson's Chi-squared test for categorical data were used to evaluate differences between female and male participants. Linear regression analysis (linear mixed effect model) was performed to investigate if characteristics of paranoid beliefs significantly explain the perceived attractiveness ratings of the dynamic face stimuli. We used an alpha level of 0.05 for all statistical tests.

2.5. Imaging data analysis

The pipeline of the imaging data analysis by using behavioral responses (attractiveness rating) and participants characteristics (demographics and paranoid beliefs) will be addressed in detail in the following sections (see Fig. 2 for an overview).

2.5.1. Imaging data acquisition

The experiments were performed at the Institute of Diagnostic and Interventional Neuroradiology, Inselspital, University of Bern on a 3T Siemens Magnetom Prisma scanner (Erlangen, Germany). Prior to the MRI experiment, participants received a short instruction about the task. fMRI data was acquired during the performance of the face perception task with a BOLD (Blood Oxygen Level-Dependent) T2*-weighted echo-planar imaging (EPI) sequence (48 axial slices, Repetition time/echo time (TR/TE) = 1000/30 ms, flip angle = 80°, slice thickness = 2.4 mm, inter slice gap thickness = 0 mm, matrix size = 94 × 94, field of view (FOV) = 230 mm × 230 mm, yielding a nominal isotropic resolution of 2.4 mm × 2.4 mm × 2.4 mm, 660 volumes in 11 min. The axial slices were positioned along the anterior (AC) and posterior commissura (PC).

We additionally acquired a gradient field map (B0) with a double-echo spoiled gradient-echo sequence in order to account for potential geometric distortions caused by magnetic field inhomogeneity, and excessive magnetic field inhomogeneity, with the following settings: TR = 520 ms, TE_1 = 4.92, TE_2 = 7.38 ms, matrix size = 94 × 94, FOV = 230 mm × 230 mm, voxel size: 2.4 × 2.4 × 2.4 (0 mm gaps), flip angle 60°, 48 axial slices positioned to exactly align the fMRI images. The produced magnitude and phase images were subsequently used to generate a voxel displacement map (VDM) (see "pre-processing" below).

High-resolution T1-weighted structural images were obtained with a 3D magnetization-prepared rapid acquisition with a gradient echo (MPRAGE) sequence. 160 sagittal slices, TR/TE = 2300/2.98 ms, flip angle = 9°, matrix size = 256 × 256, FOV = 256 mm × 256 mm, yielding a nominal isotropic resolution of 1 mm^3 (i.e., 1 mm × 1 mm × 1 mm), with 11 min total acquisition time (Fig. 2, section A2).

2.5.2. Pre-processing

The pre-processing and analysis of the Magnetic Resonance Imaging (MRI) data was performed using Statistical Parametric Mapping (SPM12) software (Wellcome Trust Centre for Neuroimaging, University College London) in MATLAB 2017a (MathWorks, Natick, USA). The pre-processing of the MRI images included slice scan time correction, realignment and unwarp (including the pre-calculated VDM), segmentation, skull-stripping, co-registration (the fMRI images were co-registered to each subject's anatomy), normalization to the Montreal Neurological Institute (MNI) coordinate system, and spatial smoothing with an 8-mm full width at half maximum Gaussian kernel (Fig. 2, section B1).

2.5.3. 1st level GLM

To assess how perceived facial attractiveness modulates the neural activity in regions of interest (ROI), we included the attractiveness ratings into the 1st level analysis (Fig. 2, section B2). We accomplished this by performing a univariate analysis using the general linear model (GLM). All events of dynamic face stimuli presentation were included in the model, the individual face ratings of attractiveness from each participant and for presented stimuli were entered as a parametric regressor, as well as six motion parameters were included in the GLM. Onsets were defined as the start of the stimuli presentation and the constant duration regressor was set to zero (e.g. as we used an event-related design [see SPM manual for more details]). A general linear model was fitted to the data using stimulus-specific delta functions that was convolved with canonical Hemodynamic Response Function (HRF) to model the hemodynamic response behavior.

2.5.4. 2nd level & localization

2nd level analysis was performed for the parametric regressor attractiveness. Activation clusters were determined by applying family-wise error (*FWE*) correction ($t_{(98)}$ = 5.05, $p_{(FWE)}$ < .001). Masks for the functional ROIs were extracted according to the activation clusters ($n_{cluster}$ > 5) by using the XJVIEW toolbox (http://www.alivelearn.net/xjview/) (Table 2). In order to remove voxels not corresponding to the fusiform gyrus, we masked out voxels according to the anatomical definition of the occipital and fusiform gyrus border (Kim et al., 2000) (Fig. 2, section B3).

2.5.5. Beta values extraction

To be able to explain the degree of neural response modulated by perceived attractiveness, we extracted the beta values of the parametric regressor attractiveness. This was done by extracting the beta values of the parametric regressor attractiveness of the GLM from every voxel in the ROI. An average beta value for every subject per ROI was calculated (i.e., averaged over all voxels within the ROI). Positive beta values represent a neural response towards attractive faces, zero represents no neural response by attractiveness, and negative beta values represent a neural response towards unattractive faces (Fig. 2, section C1).

2.5.6. HRF extraction

To visualize the degree of neural response by the parametric modulation of perceived attractiveness, we extracted the HRF. This was accomplished by extracting the individual HRF for each voxel using the analysis method of Finite Impulse Response (FIR) (i.e., we specified post-stimulus window length of 32 s and order of the basic functions of 32). FIR represents a model-free method (e.g., no a-priori assumptions) that can be used to estimate the onset and full shape of the hemodynamic response function (HRF). In a next step, we calculated the mean response of the parametric regressor attractiveness for every attractiveness rating (from −3 to +3) separately (i.e., we looked only at responses for dynamic faces rated as +2, +1, etc.). Further, we calculated an average HRF per participant and ROI (Fig. 2, section C2).

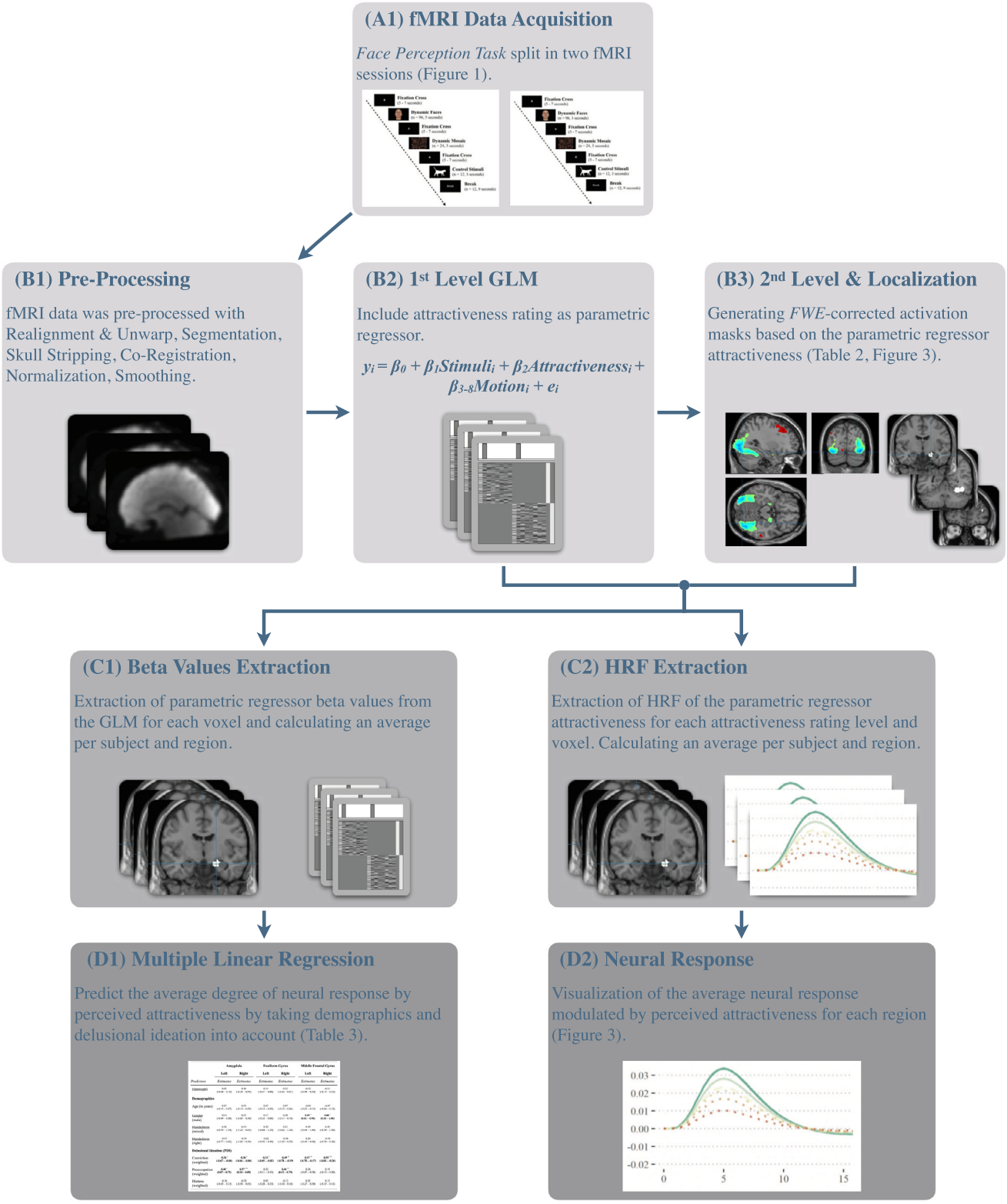

Fig 2. Schematic overview of the imaging data analysis. (A1) fMRI data acquisition for two MRI sessions using the face perception task. (B1) Pre-processing of the acquired fMRI data. (B2) 1st level analysis by including dynamic face stimuli, individual face ratings of attractiveness as parametric regressor and 6 motion parameters into the model. (B3) 2nd level analysis for the parametric regressor (attractiveness), applying FWE-correction and extracting masks based on activation clusters. (C1) Extraction of beta values from the GLM for all masks and calculating an average beta value for each participant and region of interest. (C2) Extraction of HRF values from the GLM for all masks and calculating an average HRF response for each participant, attractiveness rating level and ROI. (D1) Using multiple regression analysis to explain the degree of neural modulation (mean beta value) by perceived attractiveness with demographics (age, gender, handedness) and paranoid belief scores (conviction, preoccupation, distress). (D2) Visualization of the average parametric modulation by perceived attractiveness for each ROI. *FWE, Family-Wise Error; GLM, General Linear Model; HRF, Hemodynamic Response Function.*

Table 2
Activated network of clusters for all dynamic face stimuli of the face perception task modulated by perceived attractiveness.

Region	Abbreviation	Side	Peak MNI coordinate			Peak Intensity (*t*–Value)	Number of Voxels
			X	*Y*	*Z*		
Inferior Occipital Gyrus	IOG	L	−28	−90	−12	−13.1	2829
Middle Occipital Gyrus	MOG	L	*−0*	*−90*	*2*	*11.65*	*1402*
Fusiform Gyrus	**FG**	**L**	***−34***	***−62***	***−16***	***9.63***	***364***
Inferior Occipital Gyrus	IOG	R	38	−80	−12	−14.2	3550
Middle Occipital Gyrus	MOG	R	30	−88	2	−13.1	1431
Fusiform Gyrus	**FG**	**R**	**32**	**−64**	**−14**	**−10.8**	**664**
Middle Temporal Gyrus	MTG	L	−64	−56	−6	5.8	41
		R	64	−24	−10	6.2	189
Parietal Lobe	PL	L/R	−2	−64	52	6.6	1116
		R	56	−52	38	7.9	1217
Inferior Parietal Lobule	IPL	L	−54	54	40	6.1	397
		R	44	−44	22	5.5	7
Calcarine	CAL	L	−16	−62	18	5.5	21
		R	10	−60	18	5.3	6
Cuneus	CUN	L	−6	−94	10	6.4	200
		R	10	−92	18	6.2	194
		R	12	−86	36	5.3	7
Lingual Gyrus	LG	L	−10	−76	−8	5.6	31
		R	8	−70	−8	5.6	37
Superior Temporal Gyrus	STG	L	−64	−56	18	5.3	6
Amygdala	**AMY**	**L**	**−20**	**−6**	**−18**	**−8.8**	**107**
		R	**20**	**−6**	**−18**	**−8.1**	**164**
Cingulate	CIN	R	6	−30	38	5.5	15
Anterior Cingulate	AC	R	6	40	−8	5.8	18
Middle Frontal Gyrus	**MFG**	**L**	**−36**	**30**	**32**	**5.6**	**22**
		R	**40**	**44**	**18**	**5.6**	**32**
		R	28	28	42	6.9	578
Superior Frontal Gyrus	SFG	L	−12	56	40	−6.2	8
		L	−20	10	60	5.2	6

Note: Face-related brain activation clusters. The clusters have a threshold of t = 5.05 (p_{FWE} < .001). Brain regions marked in boldface were selected for the parametric modulation analysis. *L, left; R, right; MNI, Montreal Neurological Institute*

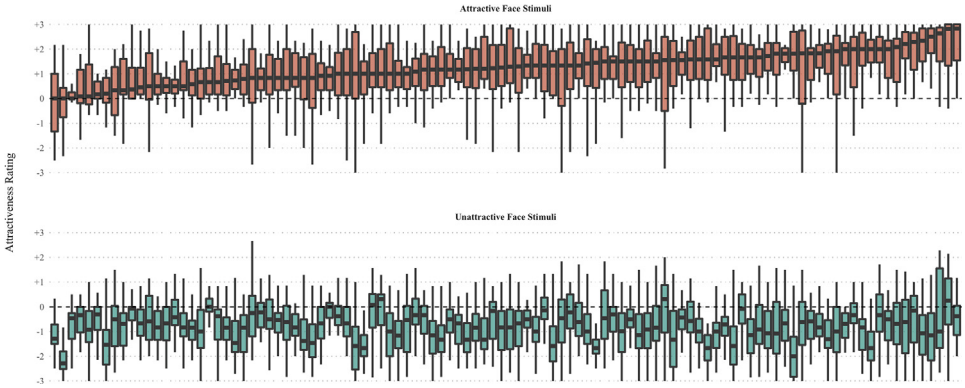

Fig 3. Display of interindividual attractiveness ratings of every participant as boxplots. Attractiveness ratings for every participant (x-axis) split by the dynamic face characteristics (unattractive & attractive) are shown and arranged according to attractiveness for the attractive stimuli. Each boxplot represents a participant, and each participant is displayed twice.

The visualization of the mean neural response by perceived attractiveness for each ROI was performed with R 3.6.1 (R Development Core Team and Development Core Team, 2011) in RStudio (version 1.2.5019) and the package ggplot2 from the tidyverse (Wickham et al., 2019) (Fig. 2, section D2).

2.5.7. Multiple regression analysis

We fitted multiple linear regression models to find out if paranoid beliefs can explain the degree of neural response by perceived attractiveness. For every ROI, we included participants' demographics (gender, age in years, handedness), and weighted paranoid belief scores (conviction, distress, preoccupation) as explanatory variables into the model. The extracted mean beta values of the parametric modulation by attractiveness for each ROI were used as the dependent variable (Fig. 2, section D1). Multiple regression analysis were performed with R 3.6.1 (R Development Core Team and Development Core Team, 2011) in RStudio (version 1.2.5019) and the R package lme4 (Bates et al., 2015). The final models fulfilled the assumptions for multiple regression analysis: values of the residuals were normally distributed, residuals showed no significant deviations, the variances of the residuals were constant, and multicollinearity was not a problem since the VIF for all explanatory variables were < 10. Effect sizes were interpreted following recommendation by Funder and Ozer (2019).

3. Results

3.1. Behavioral results

For the attractiveness ratings of dynamic faces, a score between −3 and +3 was possible. The analysis of the behavioral face ratings showed that those from the stimuli category *unattractive* had a mean rating of −1.70 (*SD* = 0.60) and those from the stimuli category *attractive* had a mean rating of 1.36 (*SD* = 0.80). The paired *t*-test suggested that the difference between attractive faces and unattractive faces (mean of differences = 3.06) is significant ($t(98) = 30.42$, 95% *CI* [2.86, 3.26], $p < .001$). As we took the individual ratings made by the

study participants of each presented dynamic face into account, Fig. 3 displays the distribution of attractiveness ratings for every participant grouped by facial characteristics (*attractive* and *unattractive*).

To investigate if paranoid beliefs can explain the attractiveness ratings of every dynamic face, we conducted mixed-effects linear regression analysis by taking demographic variables (gender, age, and handedness), paranoid belief scores (conviction, distress, and preoccupation), and random factors (participant and stimuli) into the model. The model's total explanatory power was substantial (conditional R^2 = .77) and the part related to the fixed effects alone (marginal R^2) was of .00. There were no significant effects for conviction (*beta* = 0.01, 95% *CI* [−0.07, 0.08], p = .892), preoccupation (*beta* = 0.00, 95% *CI* [−0.08, 0.08], p = .995), and distress (*beta* = -0.01, 95% *CI* [−0.09, 0.06], p = .696) on perceived attractiveness (supplementary Table S2).

3.2. Neural response of face related brain activity (BOLD-signal) by perceived attractiveness

The GLM analysis revealed 27 clusters for the activation of the dynamic faces by individual ratings of attractiveness (Table 2). The largest cluster was located in the right occipital and temporal lobe with the highest peak intensity in the right fusiform gyrus. The second cluster was in the same region in the left hemisphere, with the highest peak in the left inferior occipital gyrus (lIOG). Further, activation clusters were found of the right and left limbic lobe (including the amygdala), inferior frontal gyrus, and medial orbitofrontal cortex. Additional activation clusters were found in the precentral gyrus, and smaller activated clusters in the midbrain, hippocampus, postcentral gyrus, and inferior parietal gyrus. The results of the parametric modulation by perceived attractiveness showed an effect of attractiveness in selected regions of the emotional face-processing network. Dynamic faces evaluated as unattractive yielded a higher neural response than dynamic faces that had been rated to be more attractive (see Fig. 4).

3.3. Paranoid beliefs predict modulation of brain activation (BOLD-signal) by perceived attractiveness

Multiple linear regression analyses were conducted for each ROI to evaluate if paranoid beliefs, by controlling for participant's gender, age, and handedness, can explain the neural response by perceived attractiveness (Table 3).

The model for the left amygdala explained a not significant and weak proportion of variance (R^2 = .10, F(7, 91) = 1.51, p = .175, *adj.* R^2 = .03). Parametric modulation by attractiveness in the right amygdala explained a significant and moderate proportion of variance (R^2 = .15, F(7, 91) = 2.25, p = .037, *adj.* R^2 = .08). The effect of preoccupation was positive (*beta* = 0.57, *SE* = 0.16, 95% *CI* [0.24, 0.89], p < .001), and the effect of conviction was negative (*beta* = −0.36, *SE* = 0.15, 95% *CI* [−0.66, −0.06], p = .018), which both can be considered as significant.

For the left fusiform gyrus, the model explained a not significant and weak proportion of variance (R^2 = .07, F(7, 91) = 0.99, p = .447, *adj.* R^2 = .00), but explained a significant and moderate proportion of variance for the right fusiform gyrus (R^2 = .17, F(7, 91) = 2.67, p = .015, *adj.* R^2 = .11). For the right fusiform gyrus, there was a positive effect of preoccupation (*beta* = 0.44, *SE* = 0.16, 95% *CI* [0.12, 0.75], p = .008), as well as a negative effect of conviction (*beta* = −0.49, *SE* = 0.15, 95% *CI* [−0.78, −0.19], p = .001) which both can be considered as significant.

For the left middle frontal gyrus, the multiple regression model explained a not significant and moderate proportion of variance (R^2 = .13, F(7, 91) = 1.97, p = .067, *adj.* R^2 = .07). For the right middle frontal gyrus, we found that model explained a significant and moderate proportion of variance (R^2 = .19, F(7, 91) = 3.00, p = .007, adj. R^2 = .13). For this model, we found that the effect of conviction was negative (*beta* = −0.55, *SE* = 0.15, 95% *CI* [−0.84, −0.26], p < .001), as well as gender (male) was positive (*beta* = 0.60, *SE* = 0.23, 95% *CI* [0.14, 1.06], p = .012), and both can be considered as significant.

4. Discussion

We investigated the neural response after dynamic visual presentation of faces varying in attractiveness and interactions with subclinical paranoid beliefs in a healthy population. Dynamic face stimuli activated a network of several brain regions involved in emotional face processing. Paranoid ideas in terms of unusual beliefs of threat or power predicted more pronounced neural activation after presentation of unattractive compared to attractive faces.

The findings regarding neural activation after dynamic presentation of faces are consistent with well-described face perception and limbic circuitries (Adolphs, 2002; Foley et al., 2012; Haxby et al., 2000, 2002). In particular, we found bilateral activation of the amygdala, fusiform gyrus, and middle frontal gyrus related to the processing of faces with different attractiveness. There was a linear relationship between subjective ratings of attractiveness with the neural activation. With decreasing attractiveness, the activation of the fusiform gyrus, amygdala, and middle frontal gyrus increased. This finding is in contrast to previous research reporting non-linear, U-shaped relationships between perceived facial attractiveness and brain activation (Mattavelli et al., 2012; Mende-Siedlecki et al., 2013; Todorov et al., 2008). Compared to neutral faces both, extremely attractive and unattractive faces were linked to increased neural response in the right amygdala (Liang et al., 2010; Winston et al., 2007). This difference may be explained by studies based on computational models to investigate social perception. They showed that face typicality is a major factor for the neural modulation of the amygdala and fusiform face area. These regions responded stronger to atypical than to typical (e.g., average) faces, irrespective of their emotional valence (Said et al., 2011a; Todorov et al., 2013). Typicality of the attractive faces in our study may explain the missing activation of medial orbitofrontal cortex and nucleus accumbens described by Said et al. after presentation of exceptionally attractive faces (Said et al., 2011b).

In a functional neuroimaging study, Corlett and Fletcher (2012) reported associations between non-clinical schizotypal experiences and neural activation patterns during cognitive learning processes. In particular, the distress about unusual beliefs correlated negatively with the frontal and striatal activity to prediction error. Moreover, a recent study reported that higher paranoid beliefs are associated with elevated perfusion of limbic regions, including the hippocampus, parahippocampal gyrus, posterior cingulate cortex and thalamus, in a non-clinical population (Wolthusen et al., 2018). However, our results extend the findings of previous studies showing a significant interaction between paranoid ideation and perceived attractiveness of the presented faces on the activation of the bilateral amygdala, right fusiform gyrus, and right middle frontal gyrus. The neural response to faces with different attractiveness increased with the intensity of the subjects' paranoid ideas. Thus, to the best of our knowledge, the present study is the first neuroimaging investigation studying the functional interaction between paranoid beliefs and social cues in brain activation during face processing in healthy individuals.

In contrast to our brain imaging results, we found no behavioral effects indicating important interferences of social expectancies and education in this non-clinical population. In particular, there was no interaction between paranoid beliefs with the ratings of facial attractiveness. Previous behavioral studies investigating the associations of paranoid beliefs and social inferences are inconsistent. Haut and MacDonald (2010) showed that patients with schizophrenia rated neutral faces as more attractive but not as more trustworthy compared to healthy controls. Moreover, patients without persecutory delusions had the normal positive correlations between attractiveness and

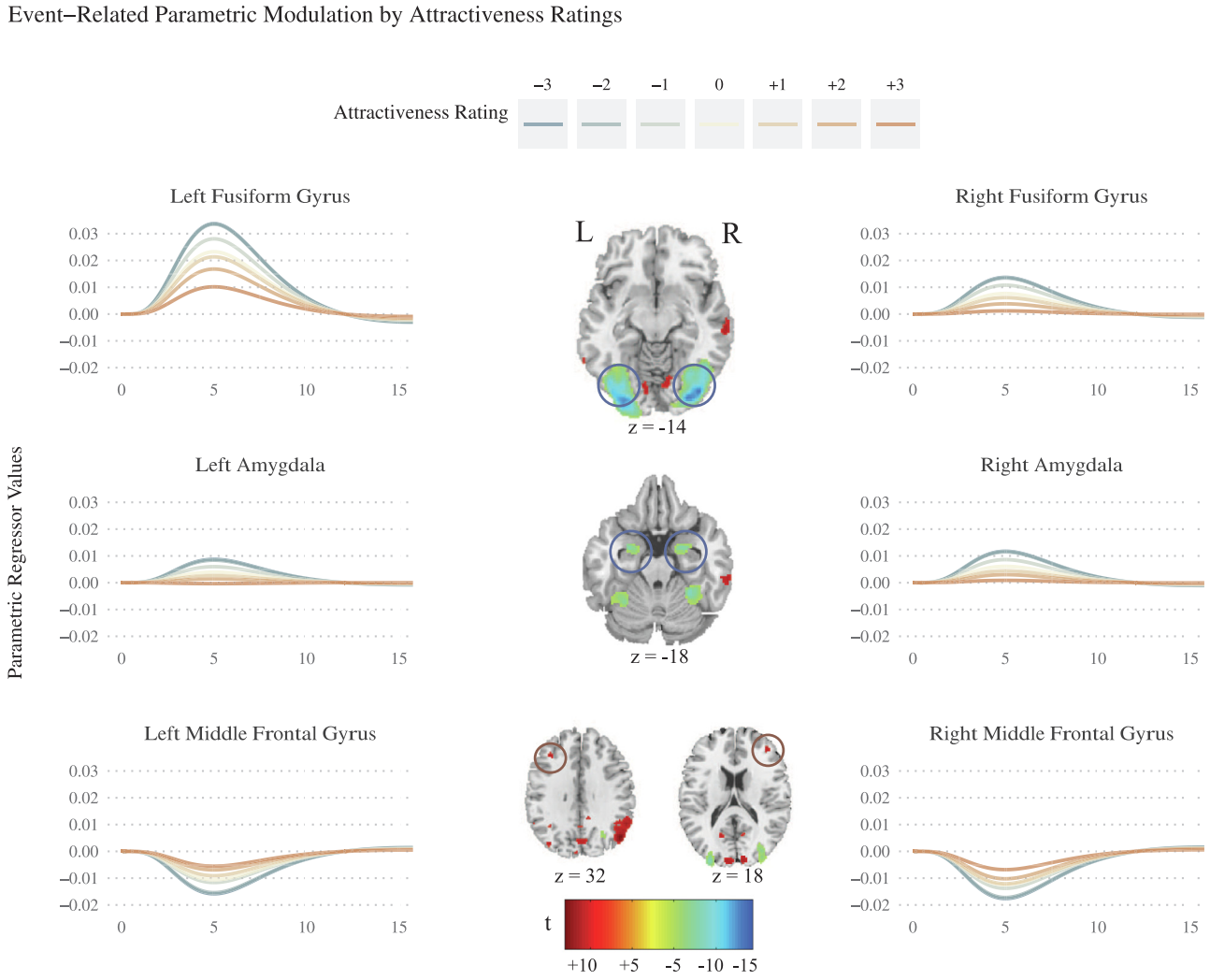

Fig 4. Brain activations pattern for the parametric modulation by perceived attractiveness in both hemispheres of three brain areas. Fusiform gyrus (left: x = −34, y = −62, z = −16; right: x = 32, y = −64, z = −14). Amygdala (left: x = −20, y = −6, z = −18; right: x = 20, y = −6, z = −18) and frontal middle gyrus (left: x = −36, y = 30, z = 32; right: x = 40, y = 44, z = 18). Results of the event-related parametric modulation analysis for the fusiform gyrus, amygdala, and middle frontal gyrus are displayed. The lines represent the average neural response by dynamic faces rated from −3 (unattractive) to +3 (attractive).

trustworthiness ratings, but this correlation disappeared with increasing delusional symptoms (Haut and MacDonald, 2010). On the other hand, McIntosh and Park (2014) showed that healthy subjects and patients with schizophrenia did not differ in social inferences (attractiveness and trustworthiness) from static emotional faces. However, with increasing paranoid beliefs, patients tended to have higher ratings of attractiveness and trustworthiness, while negative associations with paranoid beliefs were found in healthy subjects (McIntosh and Park, 2014).

The results are interesting for schizophrenia research when considered in a framework of system neuroscience. Emotion perception impairment (Kohler et al., 2010), social perception bias (Bach et al., 2009; Walther et al., 2015), and emotional dysregulation (Freeman et al., 2013; Stegmayer et al., 2014) are considered key symptoms in schizophrenia. Further, previous research with non-clinical and delusion-prone individuals provided additional evidence for an emotion and social perception dysregulation not limited to clinical populations (Amminger et al., 2012; Arguedas et al., 2006; Combs et al., 2013, 2006; Green et al., 2003). Therefore, the related basic emotional states with experiences of power or existential threat have been attributed to a dysregulation of the limbic system, which may be the common basis for different degrees of these experiences (SyNoPsis, Strik et al., 2017; Van't Wout et al., 2004). The significant interaction between delusional ideas of power or threat on the activity of face processing and limbic regions in healthy subjects in our study is consistent with the model of continuum from health to psychosis (Freeman et al., 2013; Linscott and van Os, 2010; Van't Wout et al., 2004). The absence of behavioral effects, on the other hand, indicates brain activation to be a more reliable measure of the related emotional reactivity.

Limitations of the present study include the fact that our stimulus material was generated from real faces, which were standardized for non-facial attributes (e.g., hair) and animated. This procedure may have contributed to the general emotional impact. The reduced range of attractiveness may have contributed to the linear instead of U-shaped brain response to attractiveness. Further, the findings of brain activation in regions involved in emotional face processing do not allow conclusions about the network dynamics in terms of functional connectivity between these regions. However, Foley et al. (2012) described that during the perception of emotional dynamic faces, early visual processing regions, the superior temporal sulcus, amygdala, and frontal regions are involved with increased connectivity between these regions. Finally, face attractiveness was rated outside the scanner to avoid interaction between perception and forced inference. Assuming a mood and context-dependent modulation of perceived attractiveness, this

Table 3
Results of the multiple linear regression analysis by brain region and hemisphere.

	Amygdala		Fusiform Gyrus		Middle Frontal Gyrus	
	Left *Estimates (CI)*	Right *Estimates (CI)*	Left *Estimates (CI)*	Right *Estimates (CI)*	Left *Estimates (CI)*	Right *Estimates (CI)*
Intercept	0.03 (−0.64 to 0.70)	0.30 (−0.36 to 0.95)	0.11 (−0.57 to 0.80)	0.22 (−0.42 to 0.87)	−0.32 (−0.98 to 0.34)	−0.11 (−0.75 to 0.53)
Demographics						
Age in years	0.07 (−0.13 to 0.27)	0.09 (−0.10 to 0.29)	0.07 (−0.13 to 0.28)	0.07 (−0.13 to 0.26)	−0.05 (−0.25 to 0.15)	−0.07 (−0.26 to 0.12)
Gender (male)	−0.01 (−0.49 to 0.48)	0.03 (−0.45 to 0.50)	0.17 (−0.33 to 0.66)	0.30 (−0.17 to 0.76)	0.49* (0.01 to 0.96)	**0.60*** (0.14 to 1.06)
Handedness (mixed)	0.38 (−0.59 to 1.34)	−0.31 (−1.25 to 0.63)	0.30 (−0.68 to 1.29)	0.31 (−0.62 to 1.24)	0.49 (−0.46 to 1.44)	0.58 (−0.34 to 1.50)
Handedness (right)	−0.07 (−0.77 to 0.62)	−0.34 (−1.02 to 0.34)	−0.22 (−0.92 to 0.49)	−0.38 (−1.05 to 0.29)	0.20 (−0.49 to 0.88)	−0.10 (−0.76 to 0.56)
Paranoid Belief Scores (PDI)						
Conviction (weighted)	**−0.36*** (−0.67 to −0.06)	**−0.36*** (−0.66 to −0.06)	**−0.33*** (−0.65 to −0.02)	**−0.49**** (−0.78 to −0.19)	**−0.47**** (−0.78 to −0.17)	**−0.55***** (−0.84 to −0.26)
Preoccupation (weighted)	**0.40*** (0.07 to 0.73)	**0.57***** (0.24 to 0.89)	0.22 (−0.11 to 0.55)	**0.44**** (0.12 to 0.75)	0.26 (−0.07 to 0.58)	0.19 (−0.12 to 0.50)
Distress (weighted)	−0.16 (−0.45 to 0.13)	−0.28 (−0.56 to 0.01)	0.03 (−0.26 to 0.33)	−0.12 (−0.40 to 0.16)	0.02 (−0.27 to 0.30)	0.13 (−0.15 to 0.41)
Observations	99	99	99	99	99	99
R^2/ R^2 adjusted	.104 / .035	.148 / .082	.070 / −.001	.170 / .107	.132 / .065	.188 / .125
Deviance	87.82	83.53	91.09	81.30	85.08	79.62

Note: We entered the mean beta value of the parametric regressor attractiveness from the 1st level GLM as the dependent variable into the analysis. Demographic variables and the weighted paranoid belief scores assessed with the Peters et al. Delusions Inventory (PDI) were included as explanatory variables. Significant predictors are displayed in boldface. *CI, Confidence Interval*
*p < .05 **p < .01 ***p < .001

may have reduced the accuracy of the ratings referred to the neuroimaging data.

5. Conclusion

In summary, this study showed a significant interaction between paranoid beliefs in a non-clinical population and perceived attractiveness of dynamic faces on activation of emotional face processing network, with enhanced neural response to unattractive faces. In contrast, a similar behavioral interaction of paranoid beliefs in terms of reported social evaluation on attractiveness was not found. The results support the hypothesis that paranoid beliefs are closely linked to increased activity of the limbic system. Similar results in clinical populations of paranoid syndromes suggest a common neurobiological basis.

CRediT authorship contribution statement

Stephan Furger: Conceptualization, Methodology, Investigation, Data curation, Visualization, Formal analysis, Writing - original draft. **Antje Stahnke:** Conceptualization, Methodology, Investigation, Data curation. **Francilia Zengaffinen:** Conceptualization, Methodology, Investigation, Data curation. **Andrea Federspiel:** Methodology, Data curation, Formal analysis, Writing - review & editing. **Yosuke Morishima:** Methodology, Formal analysis. **Martina Papmeyer:** Conceptualization, Methodology, Project administration. **Roland Wiest:** Resources. **Thomas Dierks:** Conceptualization, Supervision, Writing - review & editing. **Werner Strik:** Conceptualization, Supervision, Writing - review & editing.

Declaration of Competing Interest

The authors declare that they have no known competing financial interests or personal relationships that could have appeared to influence the work reported in this paper.

Acknowledgments

The authors would like to thank Fabian Steiner, Fabienne Jaun, and Chen Xie for assisting with data acquisition and data management, and Hallie Batschelet for providing language help and writing assistance for this work.

Appendix A. Supplementary data

Supplementary data to this article can be found online at https://doi.org/10.1016/j.nicl.2020.102269.

References

Adolphs, R., 2010. What does the amygdala contribute to social cognition? Ann. N. Y. Acad. Sci. 1191, 42–61. https://doi.org/10.1111/j.1749-6632.2010.05445.x.

Adolphs, R., 2008. Fear, faces, and the human amygdala. Curr. Opin. Neurobiol. 18, 166–172. https://doi.org/10.1016/j.conb.2008.06.006.

Adolphs, R., 2002. Recognizing emotion from facial expressions: psychological and neurological mechanisms. Behav. Cogn. Neurosci. Rev. 1, 21–62. https://doi.org/10.1177/1534582302001001003.

Amminger, G.P., Schafer, M.R., Papageorgiou, K., Klier, C.M., Schlogelhofer, M., Mossaheb, N., Werneck-Rohrer, S., Nelson, B., McGorry, P.D., 2012. Emotion recognition in individuals at clinical high-risk for schizophrenia. Schizophr. Bull. 38, 1030–1039. https://doi.org/10.1093/schbul/sbr015.

Arguedas, D., Green, M.J., Langdon, R., Coltheart, M., 2006. Selective attention to threatening faces in delusion-prone individuals. Cogn. Neuropsychiatry 11, 557–575. https://doi.org/10.1080/13546800500305179.

Bach, D.R., Buxtorf, K., Grandjean, D., Strik, W.K., 2009. The influence of emotion clarity on emotional prosody identification in paranoid schizophrenia. Psychol. Med. 39, 927–938. https://doi.org/10.1017/S0033291708004704.

Bach, D.R., Grandjean, D., Sander, D., Herdener, M., Strik, W.K., Seifritz, E., 2008. The effect of appraisal level on processing of emotional prosody in meaningless speech. Neuroimage 42, 919–927. https://doi.org/10.1016/j.neuroimage.2008.05.034.

Balderston, N.L., Schultz, D.H., Helmstetter, F.J., 2011. The human amygdala plays a

stimulus specific role in the detection of novelty. Neuroimage 55, 1889–1898. https://doi.org/10.1016/j.neuroimage.2011.01.034.
Bates, D., Mächler, M., Bolker, B., Walker, S., 2015. Fitting linear mixed-effects models using lme4. J. Stat. Softw. 67.
Combs, D.R., Finn, J.A., Wohlfahrt, W., Penn, D.L., Basso, M.R., 2013. Social cognition and social functioning in nonclinical paranoia. Cogn. Neuropsychiatry 18, 531–548. https://doi.org/10.1080/13546805.2013.766595.
Combs, D.R., Michael, C.O., Penn, D.L., 2006. Paranoia and emotion perception across the continuum. Br. J. Clin. Psychol. 45, 19–31. https://doi.org/10.1348/014466505X29099.
Corlett, P.R., Fletcher, P.C., 2012. The neurobiology of schizotypy: fronto-striatal prediction error signal correlates with delusion-like beliefs in healthy people. Neuropsychologia 50, 3612–3620. https://doi.org/10.1016/j.neuropsychologia.2012.09.045.
Fitzgerald, D.A., Angstadt, M., Jelsone, L.M., Nathan, P.J., Phan, K.L., 2006. Beyond threat: amygdala reactivity across multiple expressions of facial affect. Neuroimage 30, 1441–1448. https://doi.org/10.1016/j.neuroimage.2005.11.003.
Foley, E., Rippon, G., Thai, N.J., Longe, O., Senior, C., 2012. Dynamic facial expressions evoke distinct activation in the face perception network: a connectivity analysis study. J. Cogn. Neurosci. 24, 507–520. https://doi.org/10.1162/jocn_a_00120.
Freeman, D., 2007. Suspicious minds: the psychology of persecutory delusions. Clin. Psychol. Rev. 27, 425–457. https://doi.org/10.1016/j.cpr.2006.10.004.
Freeman, D., 2006. Delusions in the nonclinical population. Curr. Psychiatry Rep. 8, 191–204. https://doi.org/10.1007/s11920-006-0023-1.
Freeman, D., Dunn, G., Fowler, D., Bebbington, P., Kuipers, E., Emsley, R., Jolley, S., Garety, P., 2013. Current paranoid thinking in patients with delusions: the presence of cognitive-affective biases. Schizophr. Bull. 39, 1281–1287. https://doi.org/10.1093/schbul/sbs145.
Freeman, D., Garety, P., 2014. Advances in understanding and treating persecutory delusions: a review. Soc. Psychiatry Psychiatr. Epidemiol. 49, 1179–1189. https://doi.org/10.1007/s00127-014-0928-7.
Funder, D.C., Ozer, D.J., 2019. Evaluating effect size in psychological research: sense and nonsense. Adv. Methods Pract. Psychol. Sci. 2, 156–168. https://doi.org/10.1177/2515245919847202.
Fusar-poli, P., Placentino, A., Carletti, F., Landi, P., Allen, P., Surguladze, S., Benedetti, F., Abbamonte, M., Gasparotti, R., Barale, F., Perez, J., Mcguire, P., Politi, P., 2009. Functional atlas of emotional faces processing: a voxel-based meta-analysis of 105 functional magnetic resonance imaging studies. J. Psychiatry Neurosci. 44, 418–432.
Green, M., Williams, L., Davidson, D., 2003. Visual scanpaths and facial affect recognition in delusion-prone individuals: increased sensitivity to threat? Cogn. Neuropsychiatry 8, 19–41. https://doi.org/10.1080/713752236.
Haut, K.M., MacDonald, A.W., 2010. Persecutory delusions and the perception of trustworthiness in unfamiliar faces in schizophrenia. Psychiatry Res. 178, 456–460. https://doi.org/10.1016/j.psychres.2010.04.015.
Haxby, J.V., Hoffman, E.A., Gobbini, M.I., 2000. The distributed human neural system for face perception. Trends Cogn. Sci. 4, 223–233. https://doi.org/10.1016/S1364-6613(00)01482-0.
Haxby, J.V., Hoffman, E.A., Gobbini, M.I., 2002. Human neural systems for face recognition and social communication. Biol. Psychiatry 51, 59–67. https://doi.org/10.1016/S0006-3223(01)01330-0.
Jack, R.E., Schyns, P.G., 2015. The human face as a dynamic tool for social communication. Curr. Biol. 25, R621–R634. https://doi.org/10.1016/j.cub.2015.05.052.
Joseph, L., 2003. The emotional brain, fear, and the amygdala. Cell. Mol. Neurobiol. 23, 727–738. https://doi.org/10.1023/a:1025048802629.
Kanwisher, N., McDermott, J., Chun, M.M., 1997. The fusiform face area: a module in human extrastriate cortex specialized for face perception nancy. J. Neurosci. 17, 4302–4311.
Kim, J.J., Crespo-Facorro, B., Andreasen, N.C., O'Leary, D.S., Zhang, B., Harris, G., Magnotta, V.A., 2000. An MRI-based parcellation method for the temporal lobe. Neuroimage 11, 271–288. https://doi.org/10.1006/nimg.2000.0543.
Kohler, C.G., Walker, J.B., Martin, E.A., Healey, K.M., Moberg, P.J., 2010. Facial emotion perception in schizophrenia: a meta-analytic review. Schizophr. Bull. 36, 1009–1019. https://doi.org/10.1093/schbul/sbn192.
Liang, X., Zebrowitz, L.A., Zhang, Y., 2010. Neural activation in the "reward circuit" shows a nonlinear response to facial attractiveness. Soc. Neurosci. 5, 320–334. https://doi.org/10.1080/17470911003619916.
Lincoln, T.M., Keller, E., Rief, W., 2009. Die Erfassung von Wahn und Halluzinationen in der Normalbevölkerung: Deutsche Adaptationen des Peters et al. Delusions Inventory (PDI) und der Launay Slade Hallucination Scale (LSHS-R). Diagnostica 55, 29–40. https://doi.org/10.1026/0012-1924.55.1.29.
Linscott, R.J., van Os, J., 2010. Systematic reviews of categorical versus continuum models in psychosis: evidence for discontinuous subpopulations underlying a psychometric continuum. Implications for DSM-V, DSM-VI, and DSM-VII. Annu. Rev. Clin. Psychol. 6, 391–419. https://doi.org/10.1146/annurev.clinpsy.032408.153506.
Little, A.C., Jones, B.C., DeBruine, L.M., 2011. Facial attractiveness: evolutionary based research. Philos. Trans. R. Soc. B Biol. Sci. 366, 1638–1659. https://doi.org/10.1098/rstb.2010.0404.
Ma, D.S., Correll, J., Wittenbrink, B., 2015. The Chicago face database: a free stimulus set of faces and norming data. Behav. Res. Methods 47, 1122–1135. https://doi.org/10.3758/s13428-014-0532-5.
Mattavelli, G., Andrews, T.J., Asghar, A.U.R., Towler, J.R., Young, A.W., 2012. Response of face-selective brain regions to trustworthiness and gender of faces. Neuropsychologia 50, 2205–2211. https://doi.org/10.1016/j.neuropsychologia.2012.05.024.
McIntosh, L.G., Park, S., 2014. Social trait judgment and affect recognition from static faces and video vignettes in schizophrenia. Schizophr. Res. 158, 170–175. https://doi.org/10.1016/j.schres.2014.06.026.
Meaux, E., Vuilleumier, P., 2016. Facing mixed emotions: analytic and holistic perception of facial emotion expressions engages separate brain networks. Neuroimage 141, 154–173. https://doi.org/10.1016/j.neuroimage.2016.07.004.
Mende-Siedlecki, P., Said, C.P., Todorov, A., 2013. The social evaluation of faces: a meta-analysis of functional neuroimaging studies. Soc. Cogn. Affect. Neurosci. 8, 285–299. https://doi.org/10.1093/scan/nsr090.
Mondragón-Maya, A., Ramos-Mastache, D., Román, P.D., Yáñez-Téllez, G., 2017. Social cognition in schizophrenia, unaffected relatives and ultra-high risk for psychosis: what do we currently know? Cognición Social en Esquizofrenia, Familiares No Afectados e Individuos en Riesgo Ultra-Alto de Psicosis: ¿Qué Sabemos Actualmente? Actas Esp. Psiquiatr. 4545, 218–26218.
Montepare, J.M., Dobish, H., 2003. The contribution of emotion perceptions and their overgeneralizations to trait impressions. J. Nonverbal Behav. 27, 237–254. https://doi.org/10.1023/A:1027332800296.
Murray, G.K., 2011. The emerging biology of delusions. Psychol. Med. 41, 7–13. https://doi.org/10.1017/S0033291710000413.
O'Doherty, J., Winston, J., Critchley, H., Perrett, D., Burt, D.M., Dolan, R.J., 2003. Beauty in a smile: the role of medial orbitofrontal cortex in facial attractiveness. Neuropsychologia 41, 147–155. https://doi.org/10.1016/S0028-3932(02)00145-8.
Öhman, A., 2005. The role of the amygdala in human fear: automatic detection of threat. Psychoneuroendocrinology 30, 953–958. https://doi.org/10.1016/j.psyneuen.2005.03.019.
Oosterhof, N.N., Todorov, A., 2009. Shared perceptual basis of emotional expressions and trustworthiness impressions from faces. Emotion 9, 128–133. https://doi.org/10.1037/a0014520.
Peirce, J., 2008. Generating stimuli for neuroscience using PsychoPy. Front. Neuroinform. 2, 1–8. https://doi.org/10.3389/neuro.11.010.2008.
Peirce, J., Gray, J.R., Simpson, S., MacAskill, M., Höchenberger, R., Sogo, H., Kastman, E., Lindeløv, J.K., 2019. PsychoPy2: experiments in behavior made easy. Behav. Res. Methods 51, 195–203. https://doi.org/10.3758/s13428-018-01193-y.
Peters, E., Joseph, S., Day, S., Garety, P., 2004. Measuring delusional ideation: the 21-item Peters et al. Delusions Inventory (PDI). Schizophr. Bull. 30, 1005–1022. https://doi.org/10.1093/oxfordjournals.schbul.a007116.
R Development Core Team, Development Core Team, R., 2011. R: A Language and Environment for Statistical Computing. R Found. Stat. Comput. Vienna Austria 0, {ISBN} 3-900051-07-0. https://doi.org/10.1038/sj.hdy.6800737.
Rhodes, G., Jeffery, L., Watson, T.L., Clifford, C.W.G., Nakayama, K., 2003. Fitting the mind to the world: face adaptation and attractiveness aftereffects. Psychol. Sci. 14, 558–566. https://doi.org/10.1046/j.0956-7976.2003.psci_1465.x.
Rhodes, G., Zebrowitz, L.A., Clark, A., Kalick, S.M., Hightower, A., McKay, R., 2001. Do facial averageness and symmetry signal health? Evol. Hum. Behav. 22, 31–46. https://doi.org/10.1016/S1090-5138(00)00060-X.
Rule, N.O., Moran, J.M., Freeman, J.B., Whitfield-Gabrieli, S., Gabrieli, J.D.E., Ambady, N., 2011. Face value: amygdala response reflects the validity of first impressions. Neuroimage 54, 734–741. https://doi.org/10.1016/j.neuroimage.2010.07.007.
Said, C.P., Dotsch, R., Todorov, A., 2011a. Reprint of: the amygdala and FFA track both social and non-social face dimensions. Neuropsychologia 49, 630–639. https://doi.org/10.1016/j.neuropsychologia.2011.02.028.
Said, C.P., Haxby, J.V., Todorov, A., 2011b. Brain systems for assessing the affective value of faces. Philos. Trans. R. Soc. B Biol. Sci. 366, 1660–1670. https://doi.org/10.1098/rstb.2010.0351.
Sato, W., Yoshikawa, S., 2007. Enhanced experience of emotional arousal in response to dynamic facial expressions. J. Nonverbal Behav. 31, 119–135. https://doi.org/10.1007/s10919-007-0025-7.
Schiltz, C., Rossion, B., 2006. Faces are represented holistically in the human occipito-temporal cortex. Neuroimage 32, 1385–1394. https://doi.org/10.1016/j.neuroimage.2006.05.037.
Sergent, J., Ohta, S., Macdonald, B., 1992. Functional neuroanatomy of face and object processing: a positron emission tomography study. Brain 115, 15–36. https://doi.org/10.1093/brain/115.1.15.
Stegmayer, K., Horn, H., Federspiel, A., Razavi, N., Bracht, T., Laimböck, K., Strik, W., Dierks, T., Wiest, R., Müller, T.J., Walther, S., 2014. Ventral striatum gray matter density reduction in patients with schizophrenia and psychotic emotional dysregulation. NeuroImage Clin. 4, 232–239. https://doi.org/10.1016/j.nicl.2013.12.007.
Stip, E., Letourneau, G., 2009. Psychotic symptoms as a continuum between normality and pathology. Can. J. Psychiatry 54, 140–151. https://doi.org/10.1177/070674370905400302.
Strik, W., Stegmayer, K., Walther, S., Dierks, T., 2017. Systems neuroscience of psychosis: mapping schizophrenia symptoms onto brain systems. Neuropsychobiology 75, 100–116. https://doi.org/10.1159/000485221.
Sutherland, C.A.M., Oldmeadow, J.A., Santos, I.M., Towler, J., Michael Burt, D., Young, A.W., 2013. Social inferences from faces: ambient images generate a three-dimensional model. Cognition 127, 105–118. https://doi.org/10.1016/j.cognition.2012.12.001.
Todorov, A., Mende-Siedlecki, P., Dotsch, R., 2013. Social judgments from faces. Curr. Opin. Neurobiol. 23, 373–380. https://doi.org/10.1016/j.conb.2012.12.010.
Todorov, A., Said, C.P., Engell, A.D., Oosterhof, N.N., 2008. Understanding evaluation of faces on social dimensions. Trends Cogn. Sci. 12, 455–460. https://doi.org/10.1016/j.tics.2008.10.001.
Trautmann, S.A., Fehr, T., Herrmann, M., 2009. Emotions in motion: dynamic compared to static facial expressions of disgust and happiness reveal more widespread emotion-specific activations. Brain Res. 1284, 100–115. https://doi.org/10.1016/j.brainres.2009.05.075.
Van't Wout, M., Aleman, A., Kessels, R.P.C., Larøi, F., Kahn, R.S., 2004. Emotional

processing in a non-clinical psychosis-prone sample. Schizophr. Res. 68, 271–281. https://doi.org/10.1016/j.schres.2003.09.006.
Walther, S., Stegmayer, K., Sulzbacher, J., Vanbellingen, T., Müri, R., Strik, W., Bohlhalter, S., 2015. Nonverbal social communication and gesture control in schizophrenia. Schizophr. Bull. 41, 338–345. https://doi.org/10.1093/schbul/sbu222.
Wickham, H., Averick, M., Bryan, J., Chang, W., McGowan, L., François, R., Grolemund, G., Hayes, A., Henry, L., Hester, J., Kuhn, M., Pedersen, T., Miller, E., Bache, S., Müller, K., Ooms, J., Robinson, D., Seidel, D., Spinu, V., Takahashi, K., Vaughan, D., Wilke, C., Woo, K., Yutani, H., 2019. Welcome to the tidyverse. J. Open Source Softw. 4, 1686. https://doi.org/10.21105/joss.01686.
Winston, J.S., O'Doherty, J., Kilner, J.M., Perrett, D.I., Dolan, R.J., 2007. Brain systems for assessing facial attractiveness. Neuropsychologia 45, 195–206. https://doi.org/10.1016/j.neuropsychologia.2006.05.009.
Wolthusen, R.P.F., Coombs, G., Boeke, E.A., Ehrlich, S., DeCross, S.N., Nasr, S., Holt, D.J., 2018. Correlation between levels of delusional beliefs and perfusion of the hippocampus and an associated network in a non-help-seeking population. Biol. Psychiatry Cogn. Neurosci. Neuroimag. 3, 178–186. https://doi.org/10.1016/j.bpsc.2017.06.007.
Zebrowitz, L.A., Hall, J.A., Murphy, N.A., Rhodes, G., 2002. Looking smart and looking good: facial cues to intelligence and their origins. Personal. Soc. Psychol. Bull. 28, 238–249. https://doi.org/10.1177/0146167202282009.
Zebrowitz, L.A., Montepare, J.M., 2008. Social psychological face perception: why appearance matters. Soc. Personal. Psychol. Compass 2, 1497–1517. https://doi.org/10.1111/j.1751-9004.2008.00109.x.
Zebrowitz, L.A., Rhodes, G., 2004. Sensitivity to "Bad Genes" and the anomalous face overgeneralization effect: cue validity, cue utilization, and accuracy in judging intelligence and health. J. Nonverbal Behav. 28, 167–185. https://doi.org/10.1023/B:JONB.0000039648.30935.1b.